Oil & Natural Gas Technology

DOE Award No.: DE-FE0010406
DUNS No.: 170230239

Quarterly Research Performance Progress Report (Period ending 9/30/2013)

CONTROLS ON METHANE EXPULSION DURING MELTING OF NATURAL GAS HYDRATE SYSTEMS: TOPIC AREA 2

Project Period (10/1/2012 to 9/30/2013)

Submitted by:
Peter B. Flemings

Peter B. Flemings
Signature

The University of Texas at Austin
101 East 27th Street, Suite 4.300
Austin, TX 78712-1500
e-mail: pflemings@jsg.utexas.edu
Phone number: 512-475-9520

Prepared for:
United States Department of Energy
National Energy Technology Laboratory

October 30, 2013

Office of Fossil Energy

1 ACCOMPLISHMENTS:

1.1 What are the major goals of the project?

The project goal is to predict, given characteristic climate-induced temperature change scenarios, the conditions under which gas will be expelled from existing accumulations of gas hydrate into the shallow ocean or directly to the atmosphere. When those conditions are met, the fraction of the gas accumulation that escapes and the rate of escape shall be quantified. The predictions shall be applicable in Arctic regions and in gas hydrate systems at the up dip limit of the stability zone on continental margins. The behavior shall be explored in response to two warming scenarios: longer term change due to sea level rise (e.g. 20 thousand years) and shorter term due to atmospheric warming by anthropogenic forcing (decadal time scale).

Milestone Description	**Planned Completion**	**Actual Completion**	**Verification Method**	**Comments (progress toward achieving milestone, explanation of deviation from plan, etc.)**
1.A 1-D simulation of gas hydrate dissociation in natural systems.	9/30/2013		Report	We have simulated hydrate dissociation due to temperature change with a fully coupled model and we are currently further exploring this behavior.
1.B 1-D Simulation of gas hydrate dissociation in laboratory controlled conditions.	3/31/2014		Report	We have performed numerical simulations to guide and design our experimental work to be performed in July and August, 2013.
1.C Model-based determination of conditions required for gas not to reach seafloor/atmosphere from dissociating hydrate accumulation.	3/31/2014		Quarterly Report	We have not yet begun to address this issue.
1.D Determination of what hydrate reservoirs are at three-phase equilibrium.	12/30/2013		Report	We have developed an approach to characterize the in situ stability of hydrate reservoirs. We are applying approach to known reservoirs. See comments below
1.E Demonstrate ability to create and dissociate methane hydrate within sediment columns under conditions analogous to natural systems.	9/30/2013		Report	We have developed thermistor strings for use in experimental device. We have performed experiments in summer 2013 demonstrating the ability to create and dissociate hydrate three phase stability without adding the additional complexity of cooling from above or below.
2.A 1-D simulation of gas expulsion into hydrate stability	9/29/2014		Report	Preliminary simulations produced

zone.				
2.B Determination of conditions for which gas expulsion into hydrate-stability zone is self-limiting.	12/29/2014		Report	
2.C Demonstration of reaction transport experiment where gas invades hydrate stability zone and creates three phase stability.	9/30/2014		Quarterly Report	Currently developing/refining remote sensing technologies. Refining experimental design based on numerical simulation
2.D Demonstrate a 2D simulation of hydrate dissociation and gas expulsion.	3/31/2015		Report	

1.2 What was accomplished under these goals?

1.2.1 Task 1: Project Management and Planning:

In the last quarter, one post-doctoral scientist, and two graduate students worked on both experimental analysis and theoretical results. We now have 2 students and one post-doctoral scientist working full time on the project, in addition to PI's Flemings and Bryant, Subcontractor Kneafsey, and lab scientists Peter Polito and Donnie Brooks are working on the project. We have continued to have bi-monthly meetings with LBNL and between the Department of Geological Sciences and the Dept. of Petroleum and Geosystems Engineering. We also sent two of our scientists to work with LBNL on experimental results. Our focus over the quarter has been twofold: 1) design and perform our initial experiments and 2) continue one dimensional modeling at the lab and field scale simulating hydrate melting.

1.2.2 Task 2: Conceptual and Numerical Model Development -1D:

Subtask 2.1 - Dissociation of 1D vertical hydrate accumulation
Subtask 2.2 - Apply 1D model to laboratory experiment
Subtask 2.3 - 1D models of natural examples
Subtask 2.3.1 Hydrate accumulations below permafrost
Subtask 2.3.2 - 1D model application to deposits near up-dip limit of stability zone on continental margins

Our progress under Task 2 is described below. We have developed a fully coupled 1D hydrate model. We have been performing simulations described in Subtask 2.1, 2.2, 2.3 and 2.3.2. These are described below and in the experimental section.

1.2.2.1 1-D Warming simulations (Subtask 2.1, 2.3, 2.3.2)

We model the dissociation of methane hydrate due to a bottom water temperature change that is sufficient to dissociate all hydrate in the system. We then analyze the basic system response.

In this simulation we initiate a bottom water temperature change of 5 degrees (Fig. 1). We assume an 800 meter water depth, an initial seafloor temperature of 5 degrees, and a porewater salinity equal to seawater (.035 kg/kg). Temperature follows a smooth gradient that is controlled by the constant basal heat flux (55 mW m^{-2}). Hydrate is assumed to occupy a zone 10 meters thick with a saturation of 34%. A 30 meter gas column is trapped beneath the methane hydrate layer. Water pressure is nearly hydrostatic. The upper temperature boundary is set to 10 degrees C., 5 degrees higher than the initial condition. This new temperature means that at equilibrium conditions with seawater salinity and a steady state temperature gradient, the new base of the hydrate stability zone will lie above the seafloor (i.e. no hydrates will be stored).

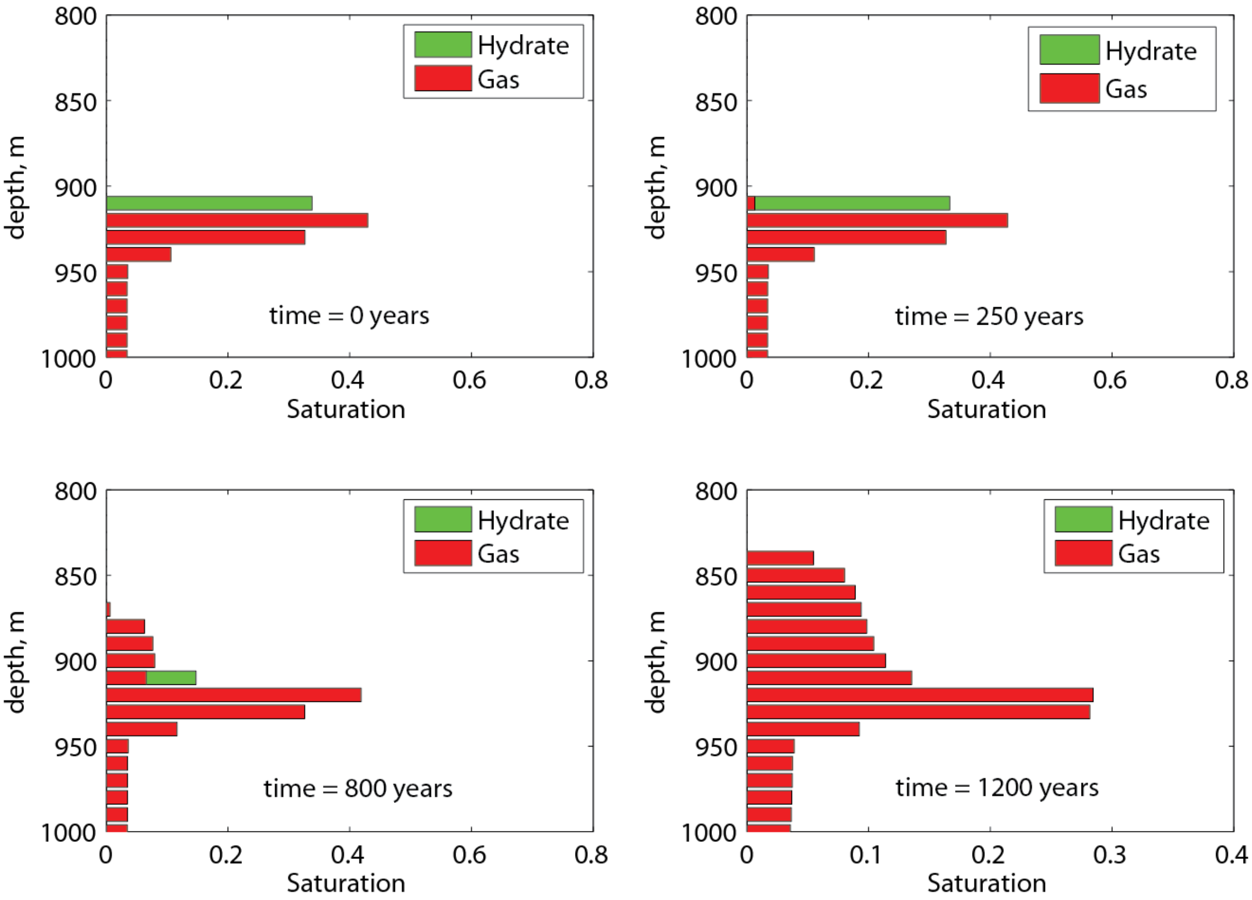

Figure 1: Gas and hydrate saturations versus depth at various stages of the dissociation process. Time increases L-R, then down. For the first 200 years, hydrate is still stable and warming has not propagated to the hydrate depth (upper left). At ~200 years, hydrate begins to dissociate and gas saturation increases locally. Between 200-1100 years, gas pressure increases and gas saturation exceeds the hydrate saturation (lower left). At ~1200 years, all hydrate has dissociated.

The temperature profile gradually equilibrates to this new temperature boundary condition (Fig. 2). At first (t = 0 and 200 years), there is a temperature reversal beneath the seafloor; the inflection point becomes deeper with time. Once dissociation begins, the latent heat balances the warming from above until all of the hydrate has dissociated. The resulting temperature profile is approximately bilinear with the kink point located where the hydrate is dissociating. The stability temperature increases slightly (note the slight shift of the temperature line just above the BSR at 500 and 800 years, Fig. 2) due to the combined effect of freshening (due to hydrate melting) and increased pressure. After approximately 1100 years, all of the hydrate has dissociated and the temperature profile becomes smooth again.

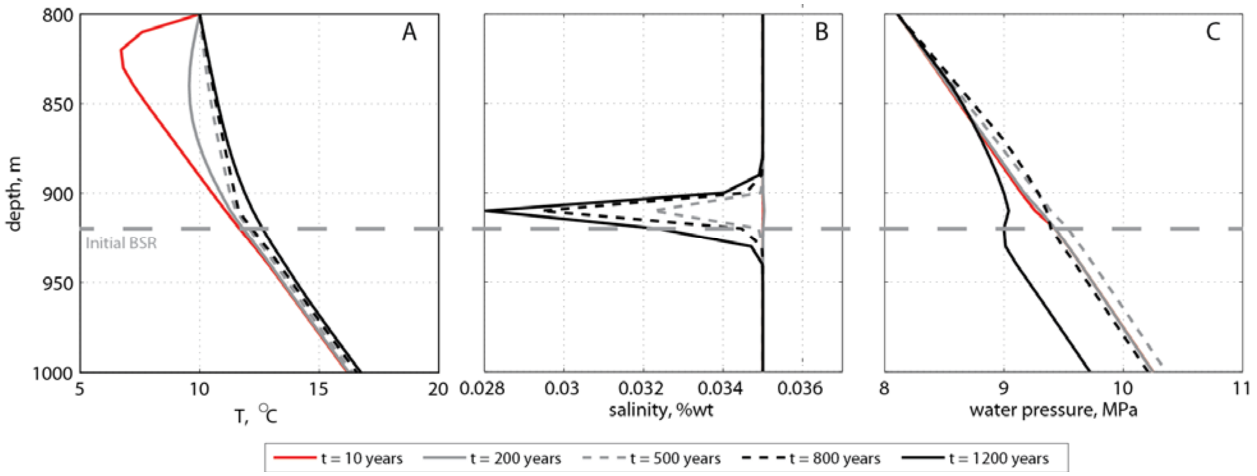

Figure 2: Temperature, salinity and pressure evolution versus depth due to bottom water increase of 5 degrees C at t=0. A) The red line records the temperature profile after 10 years. Subsequent lines show the temperature evolution during hydrate dissociation. The black line (1200 years) is shortly after all hydrate has dissociated (Fig. 7). At 200 years, temperature increase hits the hydrate layer and dissociation begins. B) The salinity is initially equal to seawater salinity and is progressively freshened during hydrate dissociation. C) Hydrate begins dissociating around 200 years and ends dissociating at 1100 years. During dissociation water pressure increases above hydrostatic. A dramatic drop in pressure occurs after complete dissociation as the gas moves upwards and vacates the pores.

Two concurrent processes affect the stability temperature during hydrate dissociation. First, pore water freshening during hydrate melting occurs as salt-free water is introduced. There is little water flux and salt diffusion is slow, so the freshening happens locally (Fig. 2b). Second, the pore pressure increases due to volume expansion during hydrate dissociation (Fig. 2c). A maximum overpressure of 190 kPa occurs at 600 years after the perturbation. This increase in pore pressure is a generic result of the dissociation process. Thus, we would expect increases in pore pressure at any depth where hydrate is present and undergoing dissociation. The magnitude of overpressure will depend on both the amount of hydrate in place initially, the rate of warming, and the permeability and compressibility of the sediment.

The overall picture of the hydrate dissociation process is as follows (Figure 1, 2). Warming at the seafloor propagates downward eventually elevating the temperature at the hydrate location to the local stability temperature. This causes dissociation. The temperature hovers close to the stability temperature for several hundred years, but adjusts very slightly according to changes in pressure and salinity at depth. Once enough hydrate dissociates, the gas buildup below the hydrate can freely flow upward and a zone with gas and hydrate exists. Eventually all of the hydrate dissociates and the pressure drops. There is a large decrease in salinity and gas saturations are quite high.

1.2.2.2 Comparisons between model simulation and laboratory measurement (Subtask 2.2)

In this section, we compare the gas, water and hydrate saturations and methane gas consumption between laboratory measurements and analytical predictions. The analytical predictions use the analytical solution developed in previous report, which is based on mass conservation of salt, fresh water and methane, and gas, water and hydrate three phase equilibrium.

Fig. 3 shows the accumulated methane gas consumption during the hydrate formation and dissociation process. In Fig. 3, the line marked by squares is the measured methane gas consumption, which has already been corrected for leakage during the experiment. The line marked by triangles is the analytically calculated methane gas consumption during the experiment. The dashed line is the methane gas consumption due to the temperature change in the sediment. T2 is the temperature measured on the sleeve. As we decrease T2 from room temperature to 10 °C, 8°C, 6°C and 4°C, the measured methane gas consumption slightly increases, which is slightly greater than that caused by the temperature change in the sediment. When T2 is decreased to 2°C, the accumulated methane gas consumption increases dramatically in one day, and then slowly reaches a constant value of about 4.8 g in the following 5 days. As we further decrease T2 to 0.5 °C, the accumulated methane gas consumption immediately increases to about 5.0 g and keeps this value for about 4.5 days. From Sep. 9, we began to increase the sample temperature from 0.5 °C to 2°C, 4 °C, 6 °C, 8 °C, 10 °C and to room temperature (about 17 °C). As can be seen in Fig. 3, the accumulated methane gas consumed by the sample decreases immediately as we increase the temperature, which means that methane hydrate dissociates very fast as the temperature increases and its kinetics is negligible. Almost 50% of the formed methane hydrate is melted on Sep. 12, when T2 is increased from 6 °C to 8 °C. When methane hydrate forms, the gas consumption rate from Aug. 28 to Aug. 29 is very fast and then becomes very slow. This is because water is limited in our experiment, the water mobility decreases as more methane hydrate is formed. During methane hydrate dissociation, the amount of methane gas released for each temperature change is determined by the three phase equilibrium condition among water, gas and hydrate. The predicted methane gas consumption is based on gas, water and hydrate three phase equilibrium condition and is about 10% higher than the measurements at 2°C and 0.5 °C. As methane hydrate forms, some brine might be blocked and isolated from methane gas which prevents further hydrate growth. The lower than equilibrium salinity in the isolated brine might cause the hydrate to dissociate in some locations and grows in some other locations, which could lead to the redistribution of methane hydrate during ageing period. During the hydrate dissociation period, the difference between the measured and calculated methane gas consumptions decreases with time.

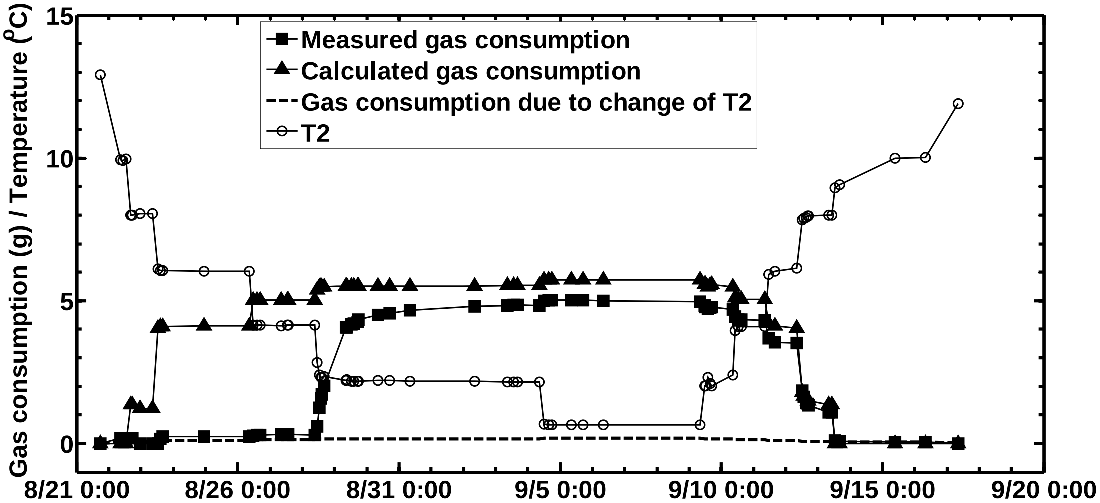

Figure 3: Comparison of measured and analytically calculated methane gas consumption during hydrate formation and dissociation process. T2 is the temperature measured on the sleeve.

Fig. 4 shows the average water, gas and hydrate saturations calculated from the measured methane gas consumption shown in Fig. 3 (1 volume of methane hydrate formation corresponds to about 2.13 volumes of methane gas consumption in this experiment). Fig. 4 also shows the predicted saturations and salinity during the experiment. The calculated final hydrate saturations are about 47% and 49% at 2 °C and 0.5 °C, respectively; while the predicted maximum hydrate saturations at three phase equilibrium are 53% and 55%, respectively, at those temperatures. The difference between the calculated and predicted saturations might be caused by the isolation of brine from methane gas, which prevents further hydrate growth. The calculated final water saturations at 2 °C and 0.5 °C are about 6% higher than those at three phase equilibrium condition. The predicted and calculated gas saturations at those temperatures match well very each other. The salinity increases with the hydrate formation and decreases with the hydrate dissociation.

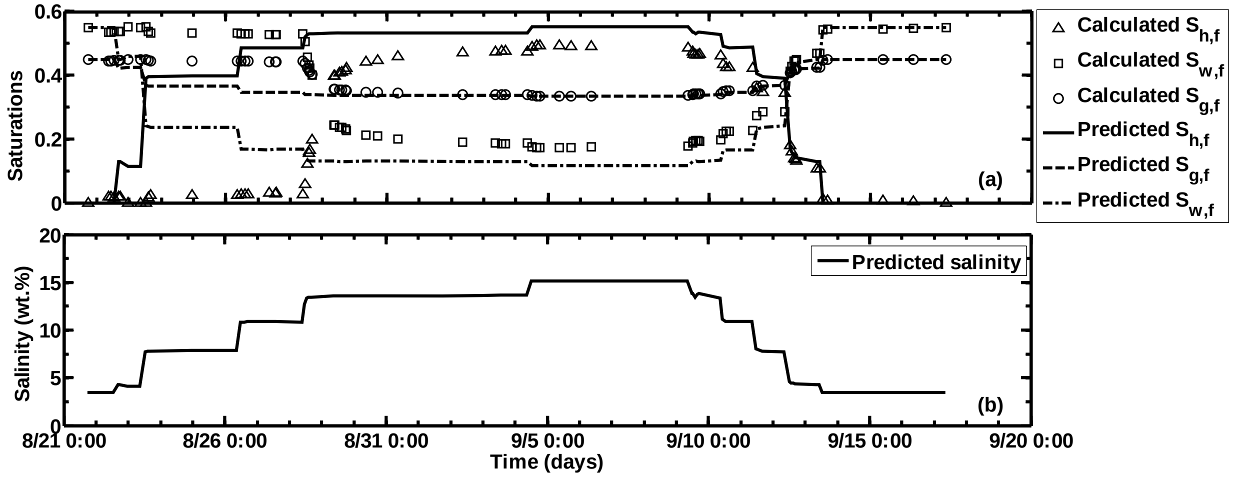

Figure 4: **(a) Comparison between the calculated average water, gas and hydrate saturations using the measured methane gas consumption and the predicted saturations using the analytical solutions in section 3. (b) The predicted average salinity during the experiment.**

1.2.3 Task 3: Categorize stability of known hydrate reservoirs:

Mallik 5L-38 Gas Hydrate Production Research Well

Since 1998, an international partnership between Canada, Japan, USA, Germany, and India has been conducting research on the production potential of onshore/offshore gas hydrate resources in the Mackenzie River delta, Northwestern Territories, Canada. The presence of a large hydrate reservoir at this site was inferred from log responses during the drilling of the L-38 well, by Imperial Oil Ltd., in 1971 (Bily and Dick, 1974). In 1998, the 2L-38 well was drilled to continue research on this hydrate reservoir. Most recently, in 2002, three wells (Figure 5) were drilled to analyze the production potential of this hydrate reservoir. Two of the wells, 3L-38 and 4L-38, were drilled as observation wells for cross-well tomography over the course of drilling and production of the main well, 5L-38 (Takahashi et al., 2005). Using the LWD and core-derived data from the Mallik 5L-38 well, we have calculated the in situ hydrate saturation and salinity and estimated the thermodynamic stability of the reservoir.

The Mallik 5L-38 well (69° 27.655’N, 134 ° 39.648’W) was drilled to an approximate depth of 1150 meters below seafloor (mbsf) through fluviodeltaic sediments. From the recovered core, the lithology at the site consisted of permafrost-cemented sediment in the first 640mbsf, underlain by water saturated, inter-bedded fine-grained and coarse-grained sediments (Haberer et al., 2005; Medioli et al., 2005).

Assuming constant geothermal (27ºC/km) and hydrostatic pressure (9.84 MPa/km) gradients, gas hydrate was determined to be thermodynamically stable between 200 – 1100 mbsf. However, according to log responses, gas hydrate was only interpreted to exist between approximately 880 – 1100 mbsf (Bily and Dick, 1974). This region was described later as the gas hydrate stability zone (GHSZ) and was further divided into 4 subzones defined by their geochemical signature, resistivity log response, and interpreted lithology (Matsumoto et al., 2005). Zone 1 extends from the top of the GHSZ to approximately 1000 mbsf and is dominated by coarse-grained material, high resistivity, and anomalously low core-derived salinity. Zone 2 goes from the base of Zone 1 to about 1065 mbsf and consists of fine-grained material, low resistivity, and seawater salinity (~550 mM Cl^-). Zone 3 extends from the base of Zone 2 to the base of the GHSZ and is identified by coarsed-grained material, high resistivity, and low salinity values. Zone 4 is defined as the sediment below the GHSZ and consists of coarse and fine-grained material, low resistivity, and seawater salinity (Figure 6).

Using LWD and core-derived data from the 5L-38 well, we implemented an iterative application of Archie's Law (Archie, 1942) and salinity correction

$$S_h = 1 - S_w = 1 - \left[\sqrt[N]{\frac{a \cdot \rho_w}{n^m \cdot \rho_t}} \right]$$

$$C_{corr} = {}^{C_0}\!/_{1 - S_h}$$

to calculate the in situ hydrate saturation (Sh) and salinity (Ccorr). We assumed the cementation exponent (m), tortuosity coefficient (a), and saturation exponent (N) were equal to 2.052, 0.745, and 4, respectively. These values were determined with a modified Pickett plot using LWD data from sediments below the GHSZ. The temperature and pressure throughout the GHSZ was determined by assuming a constant hydrostatic and geothermal gradient. An equilibrium thermodynamic model was then used to determine the salinity required to maintain three-phase equilibrium within the reservoir. Hydrate formation at Mallik 5L-38 was generally limited to Zones 1 and 3, with peak saturations between 60 and 80 percent (Figure 7A). In situ salinites were correlated with hydrate saturations and tended to decrease towards the top of the GHSZ (Figure 7B).

We estimated the stability of the reservoir by comparing the in situ salinity to the salinity required for three-phase equilibrium. We found that three-phase stability only existed within the lower 125 meters of the reservoir, excluding Zone 2, and that the difference between the in situ and three-phase salinities grew with decreasing depth, indicating greater thermodynamic stability near the top of the GHSZ. This result is supported by a study performed by (Wright et al., 2005), which took four pressure cores from different depths in the reservoir, cooled and pressurized each sample to in situ conditions and then slowly heated each to form a dissociation curve. The results showed that shallower cores required a greater temperature increase to initiate dissociation, suggesting greater thermodynamic stability.

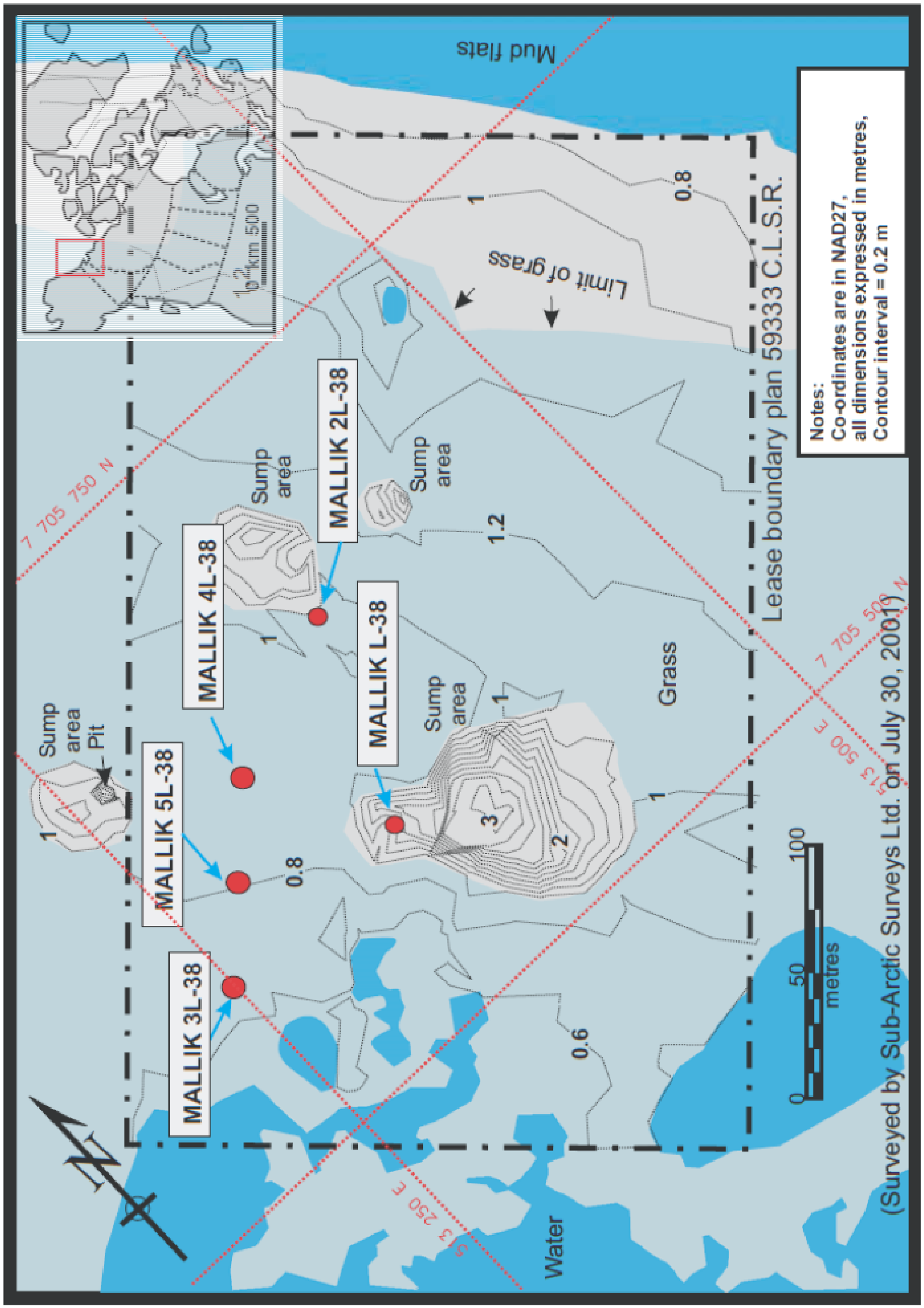

Figure 5: Map of historic Mallik drill sites located on the Mackenzie River delta. Location map and drill sites image from (Chen et al., 2005) and (Takahashi et al., 2005), respectively.

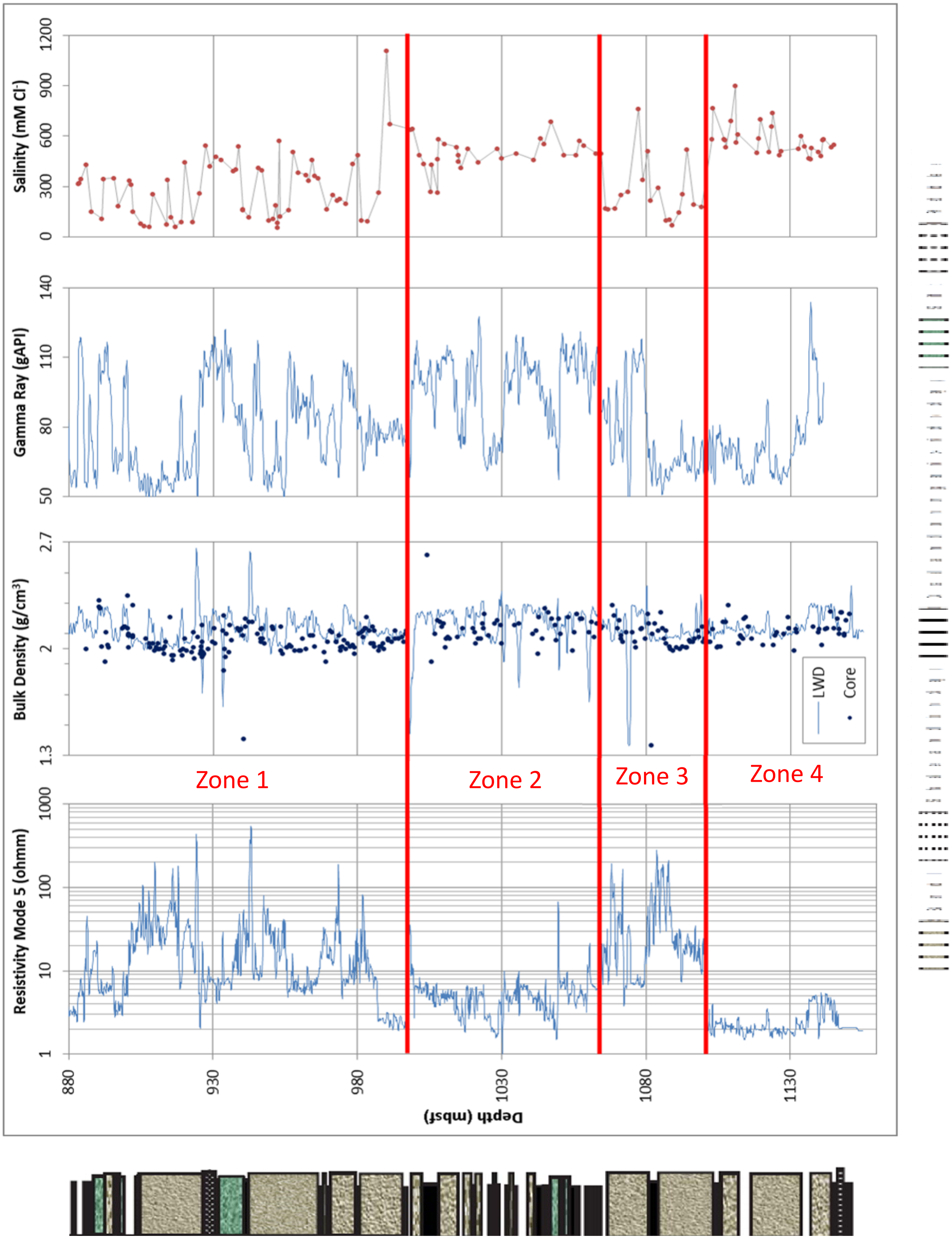

Figure 6: Salinity-defined GHSZ subzones for the Mallik 5L-38 well (Matsumoto et al., 2005) correlated with well log responses, particularly resistivity and lithology. Description of lithology provided by (Lu et al., 2005).

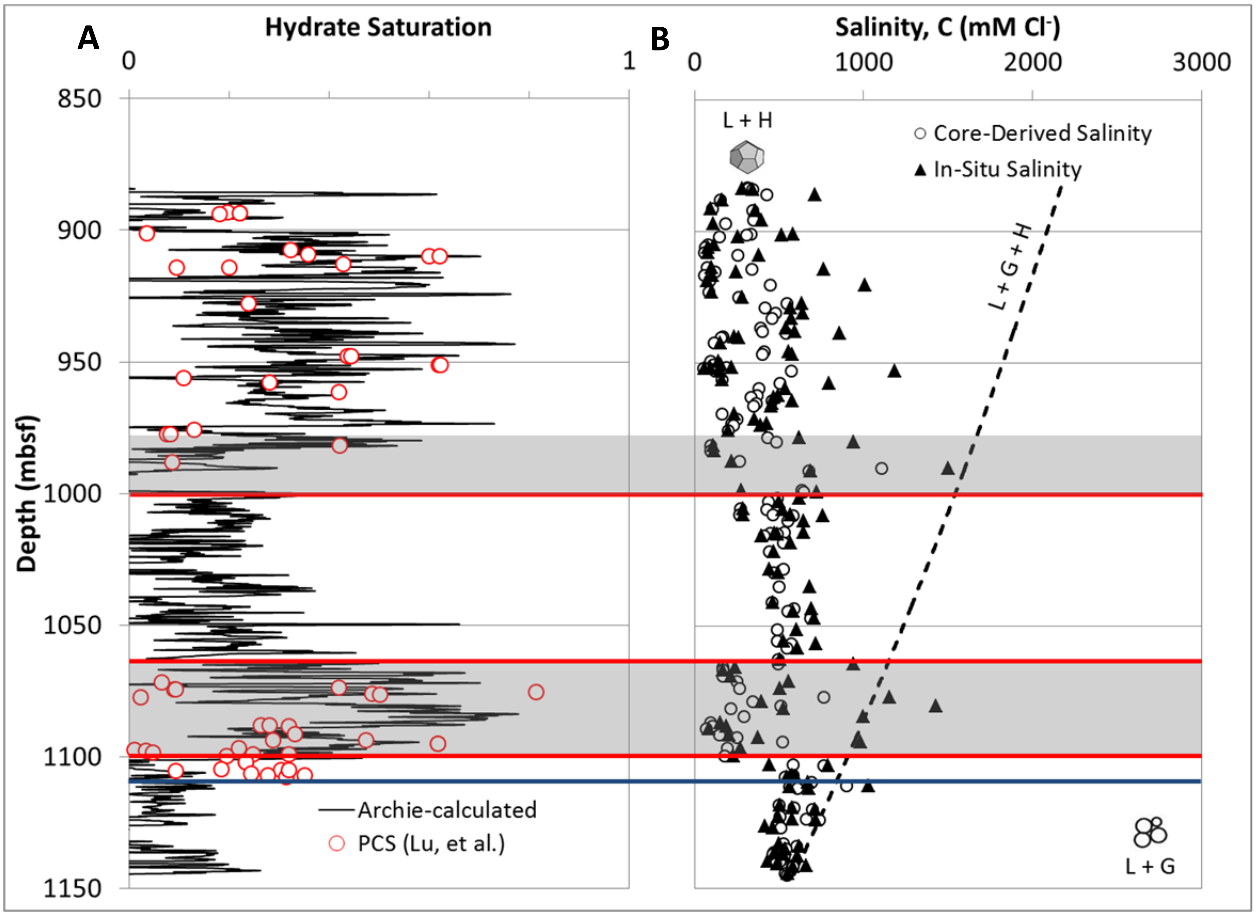

Figure 7: Results from Mallik 5L-38. A) Archie-derived hydrate saturation and hydrate saturations determined from pressure core samples (Lu et al., 2005). B) Core-derived salinity (Expedition 311 Scientists, 2006), in situ salinities, and the salinity required for three-phase stability (dashed line). Gray regions mark areas of the reservoir interpreted to be at three-phase equilibrium.

1.2.4 Task 4: Laboratory Evaluation of Hydrate Dissociation:

Subtask 4.1 - Freezing to 3 phase stability conditions, followed by melting from above
Subtask 4.2 - Freezing to L+H condition, warming from above
Subtask 4.3 - Freezing to L+H condition, warming from below

Our experimental work has been focused on four fronts: i) a literature review of previous work that is similar to the work we wish to pursue; ii) completion of development of a thermistor string at U.T. to be used in the experimental work; iii) performance and completion of our first , and iv) model simulations to define the experimental analyses we wish to pursue. We report on each of these below.

1.2.4.1 Literature review

Laboratory studies on methane hydrates formation from brine with different salinities mainly focus on three topics: the salinity effect on phase equilibrium, the amount and distribution of the hydrates formed, and the gas production from methane hydrates.

The occurrence of methane hydrates in the binary system of CH_4-H_2O has been studied extensively (De Roo et al., 1983). The experimental works were summarized in (Sun and Duan, 2005). The pioneer work to study the phase behavior of the ternary system CH_4-H_2O-NaCl is (De Roo et al., 1983). The experiments were carried out in Cailletet tubes under isobaric conditions. The temperatures at which hydrates disappear were measured for the pressure range of 2 to 11 MPa and salinity range of 0 to 0.089 mol%. An empirical equation was provided to describe the three phase (Liquid-Gas-Hydrate) equilibrium pressure as a function of temperature and salinity for a CH_4-H_2O-NaCl system. Subsequently, more experimental work was conducted to investigate the salinity effect on three phase equilibrium conditions of methane hydrates for larger pressure and salinity ranges in cells without porous media. Example works include (Maekawa et al., 1995), (Mei et al., 1996), (Kang et al., 1998), (Maekawa and Imai, 2000), (Jager and Sloan, 2001), (Kharrat and Dalmazzone, 2003), (Eichholz et al., 2004), (Atik et al., 2006), (Mohammadi et al., 2008), and (Saw et al., 2012). Besides electrolytes, the presence of various concentrations of organic hydrate inhibitors (methanol and ethylene glycol) or their mixtures with salts were also widely studied for their influence on the three phase equilibrium conditions of methane hydrates in cells (Bishnoi and Dholabhai, 1999; Dholabhai et al., 1997; Eichholz et al., 2004; Jager et al., 2002; Masoudi et al., 2005; Mohammadi and Richon, 2009, 2010; Najibi et al., 2009; Ng and Robinson, 1985).

Few studies have been conducted in porous media to investigate the phase equilibrium of methane hydrates in the presence of salts. (Østergaard et al., 2002) recorded the pressure-temperature (P-T) histories in methane hydrate dissociation for 3.5 wt% methanol aqueous solutions in confined silica glass pores of narrow distribution (30.6, 15.8 and 9.2 nm mean diameters) to investigate the methane hydrate stability suppression by capillary effects. The initial ratios of liquid volumes to pore volumes are 100% (termed saturated), 105% (termed supersaturated) and 115% (termed supersaturated), respectively. During the experiment, cell temperature was lowered until methane hydrates formation began. After hydrates formation, hydrate dissociation was initiated by raising the temperature step by step back to the initial conditions. At the end of their study, they correlated the inhibition of pore sizes to that of NaCl solutions with different mass fractions at the pressure of 10 MPa. (Liu et al., 2013) investigated the effects of different types of salts with various concentrations on the P-T stability conditions of methane hydrates in both silica sands with different grain sizes and in marine sediments sampled from South China Sea. The same conclusions as previous studies conducted in cells were reached: the presence of salts shifts the P-T curves to the left (toward higher pressure and lower temperature), and the larger the concentration, the bigger the shift.

Only a few studies experimentally examined the hydrates amount and distribution formed from brine solutions. (Yousif and Sloan, 1991) and (Yousif et al., 1991) designed experimental procedures for methane hydrates formation from 1.5 wt% NaCl solution in three different Berea sandstone cores A, B and C with different dimensions and permeabilities (8.388×10^{-14}, 9.869×10^{-14} and 3.947×10^{-13} m^2, respectively). During hydrate formation, the bath temperature was maintained at 273.7 K at a pressure always higher than the equilibrium value for a period of 4 to 34 hours. Hydrate formation was assumed to have ceased when no change in the pressure and electric resistance was observed. After equilibrium conditions were reached, one or more cycles of annealing process were performed to eliminate the pressure drop during hydrate formation and to ensure more uniform hydrate distribution along the core. After hydrate formation, hydrate dissociation was initiated by decreasing the pressure at the inlets of the cores. Three runs were conducted in core A with initial water saturation of 51.5%, 53.7% and 58.9%, respectively. Another three runs were conducted in core B with initial water saturation of 34.4%, 36.3% and 55.0%, respectively. Only one run was conducted in core C with initial water saturation of 34.5%. (Yousif and Sloan, 1991) focused on discussing the factors that influence the amount of hydrates formed and the distribution of the hydrates across the cores, including the process of annealing, the initial permeability of the cores and the initial water saturation. However, the salinity effect was not investigated. Later, (Husebø et al., 2009) conducted laboratory experiments to form methane hydrates in several sandstone cores with different geometries. The cores were all partially saturated with brine of different salinities with methane occupying the other phase. The temperature, pressure and the amount of methane injected were monitored throughout the entire experiments. They then analyzed the effect of salinity on the fill fraction, the amount of methane per available structural site in hydrates. They found that salinities lower than the regular sea water composition had negligible impact on the fill fraction of methane hydrates. However, when the salinity was higher than the sea water composition, the fill fraction significantly dropped. (Chen et al., 2009) experimentally studied the salting out phenomenon of six kinds of ions after methane hydrates formation in porous media. They found that all kinds of ionic concentrations were increased, and Ca^{2+} concentration was most significantly increased after hydrate formation.

In recent years, several laboratory experiments have been conducted to study the gas production behaviors by methane hydrates dissociation in saline water. (Li et al., 2011) conducted laboratory experiments to generate methane hydrates from synthetic brine with 2.0 wt% NaCl in natural marine sand in a closed system. After hydrates formation stopped, the dissociation was initiated by injecting hot brines. The decomposition rates of hydrates and the energy efficiencies were investigated by changing the temperature of the injected hot brine, the injection rates and time. Researchers in China University of Petroleum, Beijing and Chinese Academy of Science, Guangzhou have also conducted several laboratory experiments to investigate the methane hydrates formation in sand columns with different brine salinities, and hydrate dissociation by hot water injections, inhibitor injections and depressurization (Tang et al., 2005; Yang et al., 2012; Yang et al., 2010; Yuan et al., 2013; Yuan et al., 2011).

1.2.4.2 Thermistor string

Construction of the thermistor string is complete. It has been delivered to Dr. Kneafsey at LBNL and awaits use in upcoming experiments. The only remaining task is adapting the thermistor string data acquisition system to the Keithley DAQ used in Dr. Kneafsey's lab. This task does not pose any issues.

1.2.4.3 Experimental set-up

The initial hydrate stability experiments took place in a 2.0" diameter by 5.0" long core holder. The experiment (Figure 8) consists of a temperature controlled jacket encasing the pressure controlled cell. Within the pressure controlled cell is the confining fluid, an EPDM sleeve (containing the sample between PVC end pieces), a thermocouple attached to the outside of the EPDM sleeve, a thermocouple extending through the outlet tubing into the sample, end caps, the necessary plumbing components, and two silver/silver chloride electrodes mounted to a narrow piece of Garolite®. The electrode wires are passed through a 1/16" OD stainless steel tube and swaged to an outer connector. In this configuration, the 1/16" tube housing the electrode wires lies within the pore fluid plumbing but remains sealed from the outside environment, this allowing for conductivity data acquisition without opening the system to atmospheric conditions.

We used US Silica F-110 sand mixed with a 3.5% saline to obtain a saturation of ~50%. We increased the pore fluid (methane) pressure in 50-100 psi increments, while maintaining 50 psi effective pressure, up to 1050 psig to check for leaks. We then slowly and stepwise cooled the sample into the hydrate stability field (~to 0.5 degrees C) and form hydrate. We allowed gas to enter as hydrate forms.

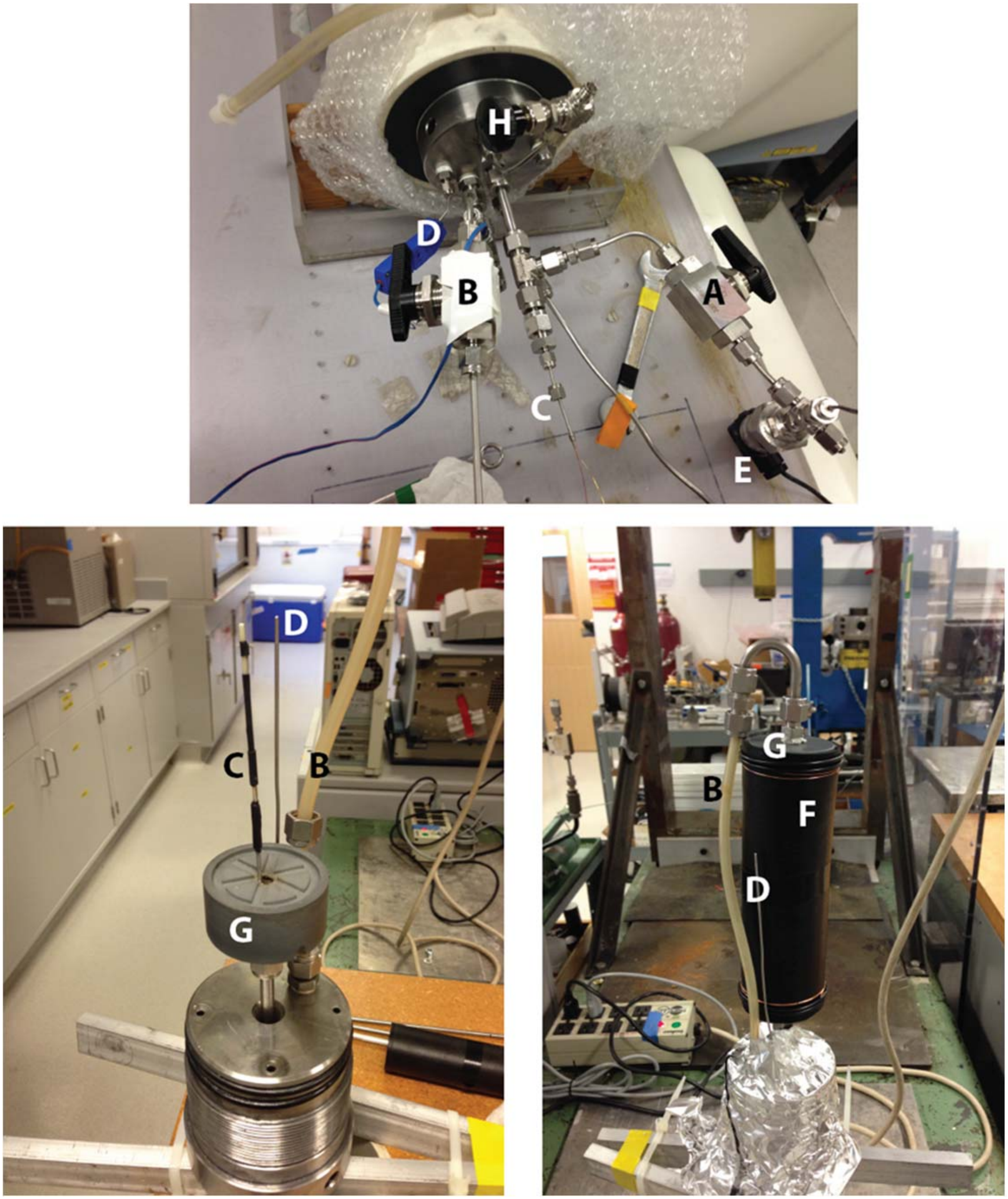

Figure 8: Experimental hydrate stability system. The pertinent components of this system are the a) pore pressure inlet, b) pore pressure outlet, c) resistivity array, d) thermocouple, e) pore pressure sensor, f) EPDM sleeve (encasing the sample), g) end caps, and h) cell pressure inlet/outlet.

1.2.4.4. Preliminary results

As the sample was cooled under constant pressure, hydrate began to form (Figure 9.). This did not occur immediately upon reaching the stability point, but a significant driving force was required. The stability temperature at the 1015 psi pressure for the salinity was approximately 8.4C. Although some hydrate formed upon lowering the temperature from 6 to 4C, significant hydrate formation occurred upon lowering the temperature to 2C, with additional hydrate forming upon dropping the temperature to 0.5C. This behavior [formation of additional hydrate upon lowering the temperature, and the presence of water (see water saturation in Figure 9)] indicate the presence of three-phase stability. Dissociation did not require the same driving force, with the dissociation occurring roughly as expected as the temperature increased.

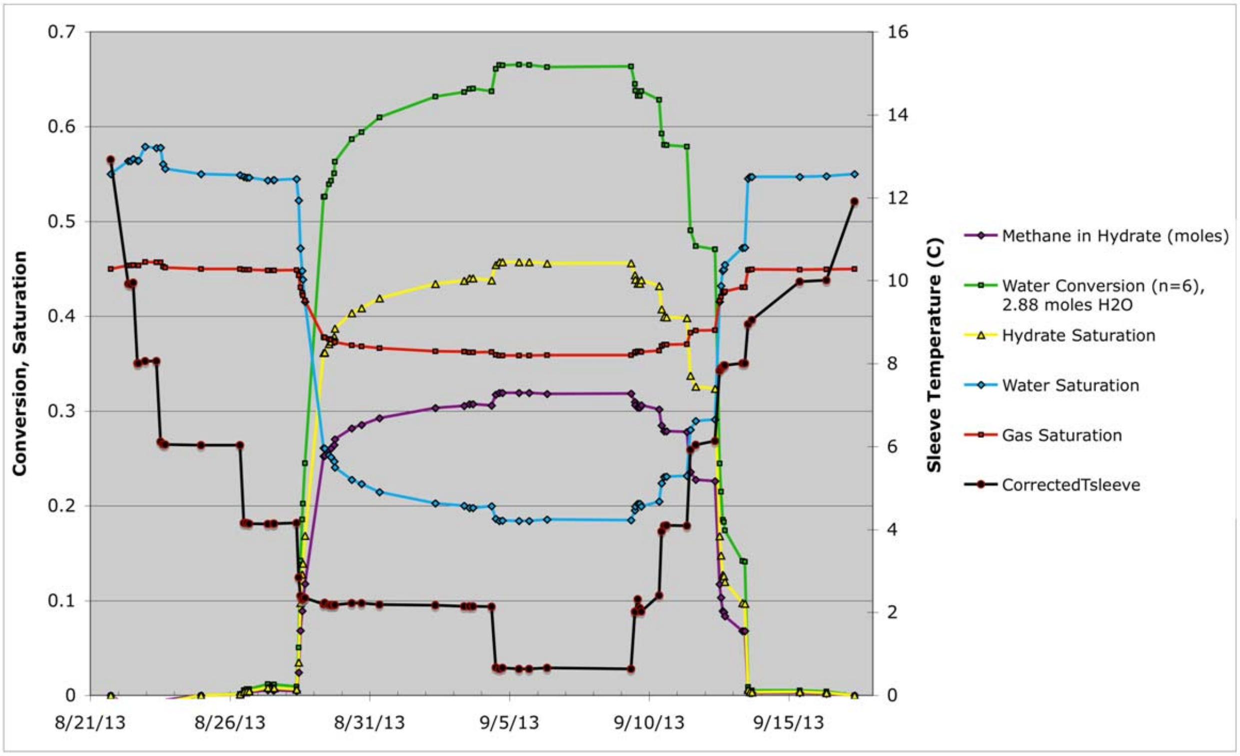

Figure 9: Water conversion to hydrate, and phase saturations during experiment.

Changes in electrical resistance (to be recomputed to resistivity upon application of the calibration curve) followed the formation and dissociation of hydrate. Resistance, hence resistivity, increased upon formation of hydrate (Figure 9). As the hydrate ripened, the resistivity decreased, likely indicating recrystallization of the hydrate towards minimizing energy. Upon dissociation, resistivity again increased, likely from freshening of the available water and then decreased again.

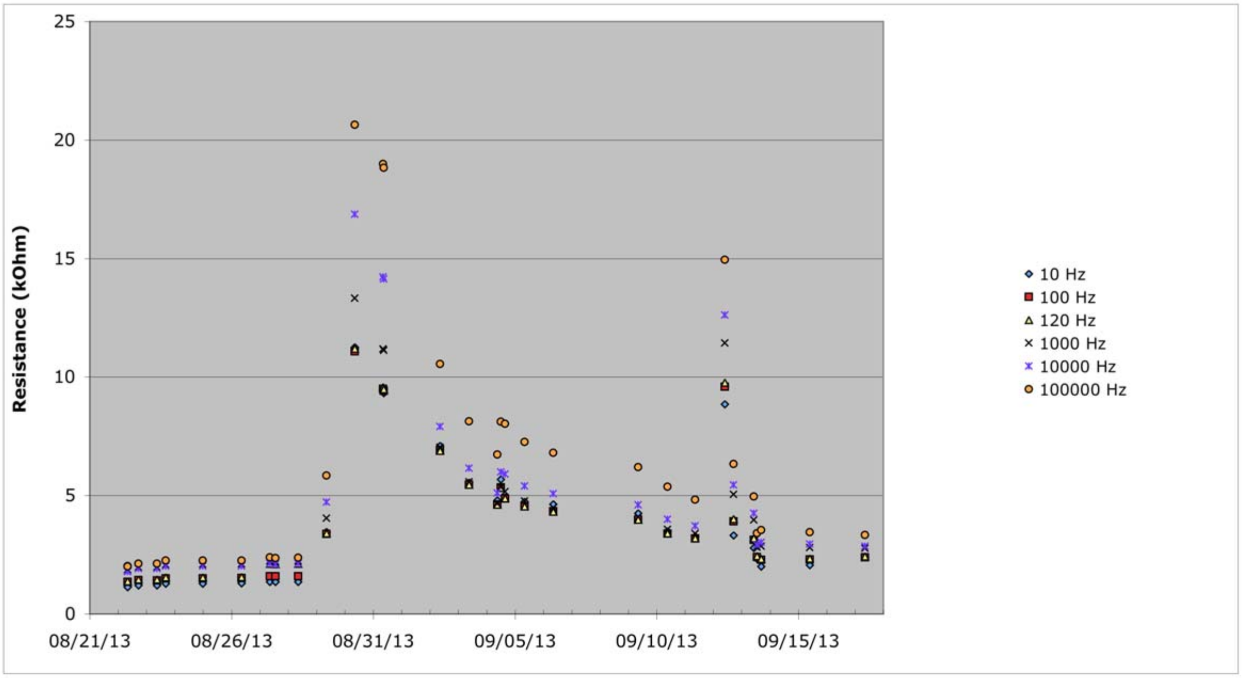

Figure 10: Electrical resistance between electrodes for the six measurement frequencies over the duration of the experiment.

X-ray computed tomography (CT) data are used to observe the three dimensional distribution of the fluids and hydrate in the sample. A cross section of the sample prior to hydrate formation is shown in Figure 11. This figure also shows the location of the electrodes, and the location of the thermocouple. The sample was packed from left to right (aligned vertically for packing), and laminations similar to natural layering are evident.

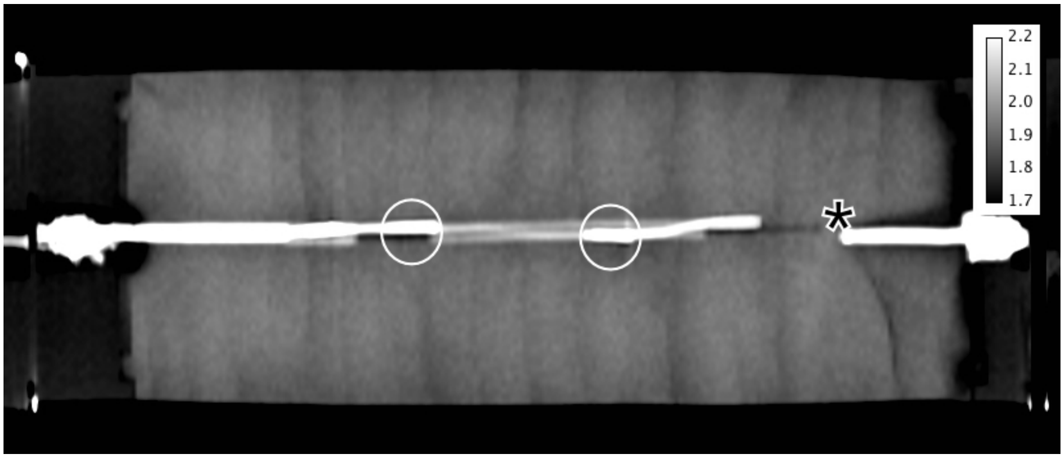

Figure 11: CT cross section of the sample. Electrodes are circled, and an * marks the end of the thermocouple.

Figure 12 shows how we look for changes in the sample using the CT data. We are able to subtract calibrated data sets to look for regions where density changes occur. Using this method, we can interrogate the data to look for trends. An example is shown in Figure 13. In this figure, we can see that the hydrate formation on the left side induced brine to flow towards that side, reducing the density on the right side. This is also shown in Figure 14, which shows cross sectional views of changes in density of the sample. Calibration and recomputation of the data is still required.

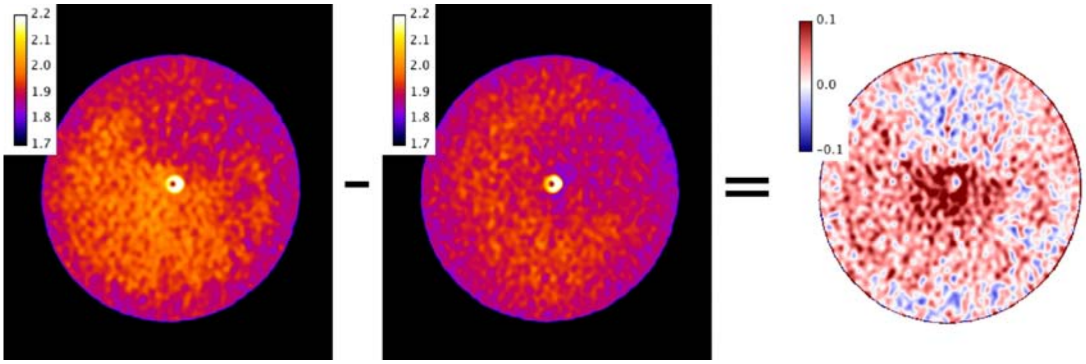

Figure 12: Calibrated density distribution of slice 135 in Scan 126 (left), slice 135 in the initial scan – 119 (center), and the difference between the two (right).

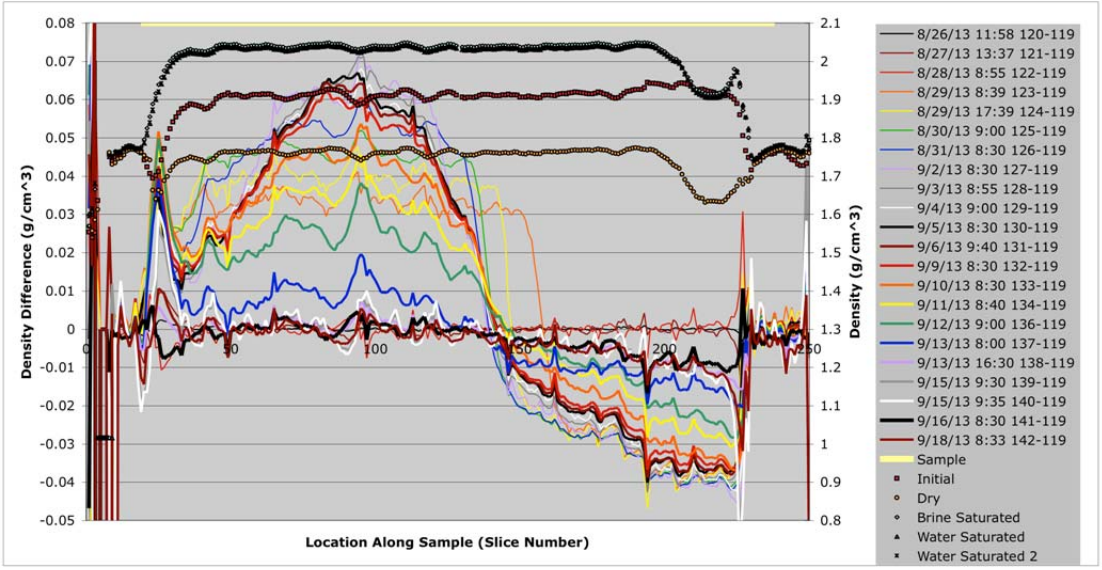

Figure 13: Density changes from the initial condition along the sample, and slice-by-slice density for specified conditions.

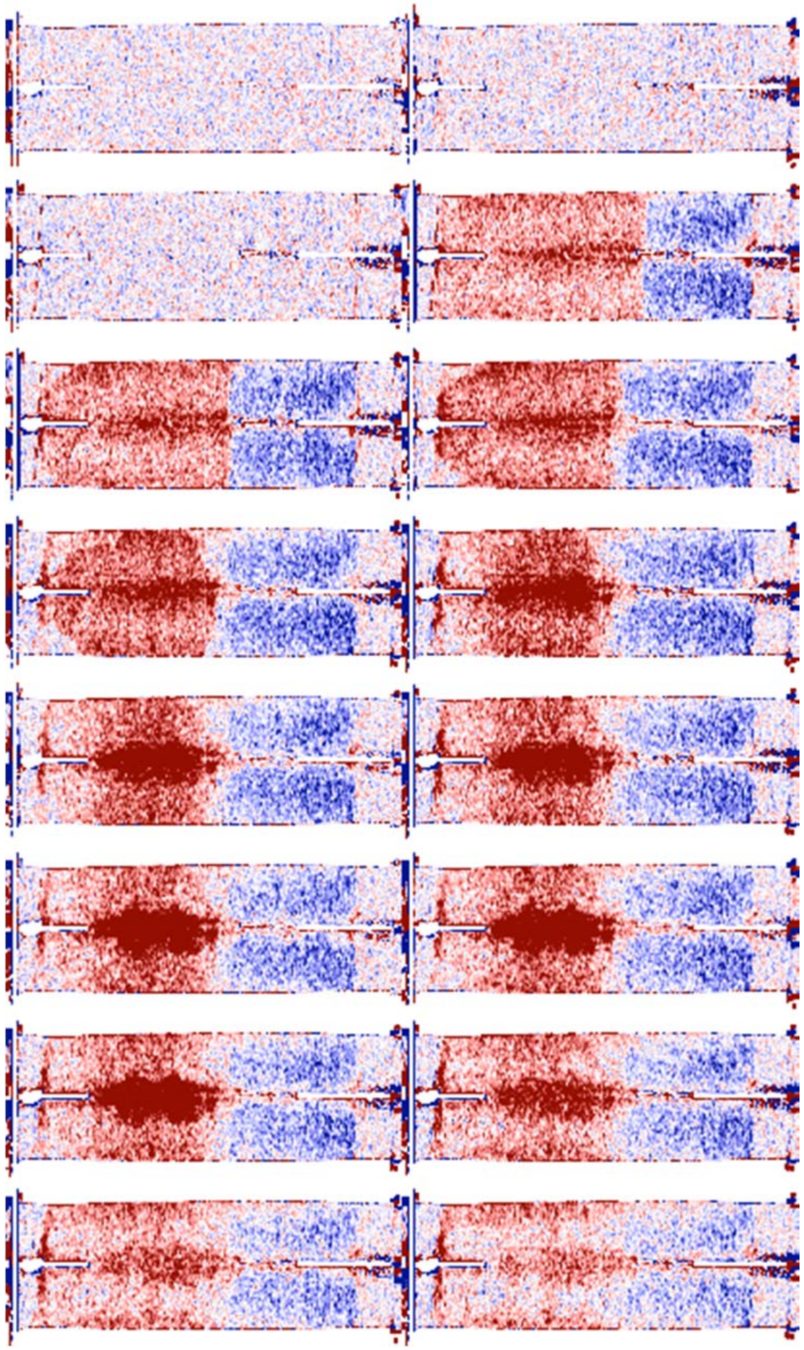

Figure 14: Cross-section views of chances in sample density over the duration of the test. Red indicates increased density, blue indicates decreased density. (left to right, top to bottom)

1.3 What opportunities for training and professional development has the project provided?

There has been strong interaction between UT and LBNL over this past quarter. Our graduate students and our post-doctoral scientist are now fully working with both institutions. There is continuous interaction between petroleum engineering and geosciences as we address this problem.

1.4 How have the results been disseminated to communities of interest?

An abstract titled, *In situ gas hydrate saturation and salinity of hydrate-bearing sediments through well log analysis*, was presented to the Society of Petrophysicists and Well Log Analysts (SPWLA) conference during June 2013.

The following abstract have been submitted to be presented at the 2013 Fall AGU Meeting:

Bhandari, A., Cronin, M., Polito, P., Flemings, P.B., Bryant, S., 2013, Mass Transport Properties in the Matrix of the Barnett Shale, Abstract submitted to be presented at 2013 Fall Meeting, AGU, San Francisco, Calif., 9-13 Dec.

Darnell, K., Flemings, P.B., 2013, Methane hydrate destabilization sensitivity to physical complexity and initial conditions in a numerical model, Abstract submitted to be presented at 2013 Fall Meeting, AGU, San Francisco, Calif., 9-13 Dec.

Kneafsey, T., Flemings, P.B., Bryant, S., You, K., Polito, P., 2013, Preliminary Experimental Examination Of Controls On Methane Expulsion During Melting Of Natural Gas Hydrate Systems, Abstract submitted to be presented at 2013 Fall Meeting, AGU, San Francisco, Calif., 9-13 Dec.

Meyer, D., Flemings, P.B., 2013, Thermodynamic state of hydrate-bearing sediments on continental margins around the world, Abstract submitted to be presented at 2013 Fall Meeting, AGU, San Francisco, Calif., 9-13 Dec.

1.5 What do you plan to do during the next reporting period to accomplish the goals?

1.5.1 Task 1: Project Management and Planning:

We will continue with bi-monthly conference calls with Berkeley. We will continue to interact directly on experimental work. We will manage travel for visitations to Berkeley. We are completing reports for the contract.

1.5.2 Task 2: Conceptual and Numerical Model Development -1D:

Subtask 2.1 - Dissociation of 1D vertical hydrate accumulation
Subtask 2.2 - Apply 1D model to laboratory experiment
Subtask 2.3 - 1D models of natural examples
Subtask 2.3.1 Hydrate accumulations below permafrost
Subtask 2.3.2 - 1D model application to deposits near up-dip limit of stability zone on continental margins

Continue model development.
We will continue addressing subtasks 2.1, 2.2, 2.3. We intend to complete all but Subtask 2.3.2 over the next 6 months.

1.5.3 Task 3: Categorize stability of known hydrate reservoirs:

Over the next three months we will complete analysis of the Mallik locations and the Mt. Elbert locations if the data are proficient. We will complete a report on these results in the next quarter. We will continue to improve the method used to process these sites and determine the thermodynamic state at each other them.

1.5.4 Task 4: Laboratory Evaluation of Hydrate Dissociation:

Subtask 4.1 - Freezing to 3 phase stability conditions, followed by melting from above
Subtask 4.2 - Freezing to L+H condition, warming from above
Subtask 4.3 - Freezing to L+H condition, warming from below

Over the next quarter we will complete the analysis of our first laboratory experiment at Berkeley, and begin developing our second laboratory setup. The needed meter-long pressure vessel has been largely preconditioned for the test, with some minor adjustments needed. We intend to be able to apply heating or cooling from either the top or bottom in the next series of tests.

2 PRODUCTS:

2.1 What has the project produced?

We have now produced a one dimensional, coupled, hydrate formation code that simulates the thermo-chemical response of a hydrate system to perturbation. We have demonstrated three phase stability through experimental analysis and we have modeled the behavior.

3 PARTICIPANTS & OTHER COLLABORATING ORGANIZATIONS:

3.1 What individuals have worked on the project?

Provide the following information for: (1) principal investigator(s)/project director(s) (PIs/PDs); and (2) each person who has worked at least one person month per year on the project during the reporting period, regardless of the source of compensation (a person month equals approximately 160 hours of effort).

Name	Peter Flemings	Steve Bryant	Tim Kneafsey	Dylan Meyer	Donnie Brooks
Project Role	Principal Investigator	Co-Principal Investigator	Co-Principal Investigator	Graduate Student	Laboratory Assistant
Nearest person month worked	.25	.25	1.25	1	1
Contribution	Advised graduate student Meyer, managed project, and recruited students. Worked with technicians for thermistor development.	Advised graduate student Meyer on analysis of models of pore space alteration due to hydrate growth and its effect on saturation exponent.	Set up experiment, ran tests, and analyzed data.	Performed analysis of thermodynamic state of 3 locations.	Built a prototype thermistor string.
Funding Support	The University of Texas	The University of Texas	Lawrence Berkeley National Lab	UTIG Fellowship	The University of Texas
Collaborated with individual in foreign country	No	No	No	No	No

Name	Peter Polito	Kris Darnell	Kehua You	Tessa Green	
Project Role	Laboratory Manager	Graduate Student	Post Doc	Project Coordinator	
Nearest person month worked	1	1	1	1	
Contribution	Participated in conference calls on experimental design. Ran experimental tests.	Performed literature review and theoretical calculation to prepare for laboratory experiments	Performed literature review and theoretical calculation to prepare for laboratory experiments	Coordinate meeting logistics, archive documents, and manage financials.	
Funding Support	The University of Texas	The University of Texas	The University of Texas	The University of Texas	
Collaborated with individual in foreign country	No	No	No	No	

3.2 What other organizations have been involved as partners?

Organization Name: Lawrence Berkeley National Lab
Location of Organization: Berkeley, CA
Partner’s contribution to the project (identify one or more)

- In-kind support (e.g., partner makes software, computers, equipment, etc., available to project staff);
- Facilities (e.g., project staff use the partner’s facilities for project activities);
- Collaborative research (e.g., partner’s staff work with project staff on the project); and

3.3 Have other collaborators or contacts been involved?

No

4 IMPACT:

4.1 What is the impact on the development of the principal discipline(s) of the project?

Geological models of gas transport and hydrate melting and solidification have suggested that free gas cannot migrate through the hydrate stability zone during melting. In contrast, we suggest that free gas can migrate through the hydrate stability zone by altering the conditions of hydrate stability to a state of three-phase equilibrium through the elevation of salinity and possibly temperature. This results in fundamentally different macro-scale behavior during melting and may result in greater gas venting than has been previously demonstrated. If this hypothesis is correct, it may engender a new generation of field and laboratory investigations to document this behavior in both the field of geosciences and petroleum engineering. Second, the project links theoretical development with laboratory modeling because the concepts can be applied at the laboratory scale as well as the field scale. The laboratory experiments to be conducted will enable validation of the mechanisms incorporated in the models. These laboratory experiments will play a key role in demonstrating the processes.

4.2 What is the impact on other disciplines?

A likely outcome of our work is a more quantitative prediction of the magnitude of methane flux from the earth to the atmosphere over human (decadal) timescales and geological timescales (10,000 years). These will serve as boundary conditions for atmospheric climate models. In turn, these results may guide policy decisions.

4.3 What is the impact on the development of human resources?

We are working at the interface of geosciences and engineering. We are coupling theory and laboratory experiments to address macro-scale geologic problems. This is training a new generation of geoscientists and engineers to think with a systems-based approach that links observation with theory.

The results are being applied in the classroom and the support is training several graduate students.

4.4 What is the impact on physical, institutional, and information resources that form infrastructure?

The project is strengthening the experimental efforts and capability at UT as it is our drop to develop sensor equipment. The project is strengthening development at LBNL where primary experimental work is occurring.

4.5 What is the impact on technology transfer?

We are presenting our research to approximately 100 industry members at our GeoFluids consortium and we will be presenting at a range of national and international meetings.

4.6 What is the impact on society beyond science and technology?

A likely outcome of our work is a more quantitative prediction of the magnitude of methane flux from the earth to the atmosphere over human (decadal) timescales and geological timescales (10,000 years). These will serve as boundary conditions for atmospheric climate models. In turn, these results may guide policy decisions.

4.7 What dollar amount of the award's budget is being spent in foreign country(ies)?

Zero percent of the award's budget is being spent in foreign countries.

5 CHANGES/PROBLEMS:

5.1 Changes in approach and reasons for change

We have made some changes in our specific experimental approaches. The original experimental tasks were described as follows:
Task 4: Laboratory Evaluation of Hydrate Dissociation:
Subtask 4.1 - Freezing to 3 phase stability conditions, followed by melting from above
Subtask 4.2 - Freezing to L+H condition, warming from above
Subtask 4.3 - Freezing to L+H condition, warming from below

However, after experimental planning and theoretical modeling over the last quarter, we decided that the most important first step in the modeling would be to 1) demonstrate the ability to create three phase conditions in the laboratory and 2) show the effects of perturbation on this material. . After establishing this capability, we would then demonstrate the effects of thermal perturbation from above or below.

We will still be able to meet our Milestone **1.E,** ' Demonstrate ability to create and dissociate methane hydrate within sediment columns under conditions analogous to natural systems.'

There are no other changes in approach to report for this reporting period.

5.2 Actual or anticipated problems or delays and actions or plans to resolve them

No problems or delays to report for this reporting period.

5.3 Changes that have a significant impact on expenditures

No changes in approach to report for this reporting period.

5.4 Significant changes in use or care of human subjects, vertebrate animals, and/or Biohazards

Nothing to report

5.5 Change of primary performance site location from that originally proposed

Nothing to report

6 BUDGETARY INFORMATION:

Baseline Reporting (10/1/12 - 6/30/13)	Budget Period 1							
	Q1		Q2		Q3		Q4	
	10/1/12 - 2/15/13		2/16/13-6/30/2013		7/1/2013-11/15/2013		11/16/2013-3/31/2014	
	Q1	Cumulative Total	Q2	Cumulative Total	Q3	Cumulative Total	Q4	Cumulative Total
Baseline Cost Plan								
Federal Share	$ 136,111.50	$ 136,111.50	$ 175,000.50	$ 311,112.00	$ 175,000.50	$ 486,112.50	$ 175,000.50	$ 661,113.00
Non-Federal Share	$ 43,568.75	$ 43,568.75	$ 43,568.75	$ 87,137.50	$ 43,568.75	$ 130,706.25	$ 43,568.75	$ 174,275.00
Total Planned	$ 179,680.25	$ 179,680.25	$ 218,569.25	$ 398,249.50	$ 218,569.25	$ 616,818.75	$ 218,569.25	$ 835,388.00
Actual Incurred Cost								
Federal Share	$ 45,506.00	$ 45,506.00	$ 54,469.00	$ 99,975.00	$ 224,568.00	$ 324,543.00	$ -	$ 324,543.00
Non-Federal Share	$ -	$ -	$ 53,337.00	$ 53,337.00	$ 17,200.00	$ 70,537.00	$ -	$ 70,537.00
Total Incurred Cost	$ 45,506.00	$ 45,506.00	$ 107,806.00	$ 153,312.00	$ 241,768.00	$ 395,080.00	$ -	$ 395,080.00
Variance								
Federal Share	$ (90,605.50)	$ (90,605.50)	$ (120,531.50)	$ (211,137.00)	$ 49,567.50	$ (161,569.50)	$ (175,000.50)	$ (336,570.00)
Non-Federal Share	$ (43,568.75)	$ (43,568.75)	$ 9,768.25	$ (33,800.50)	$ (26,368.75)	$ (60,169.25)	$ (43,568.75)	$ (103,738.00)
Total Variances	$ (134,174.25)	$ (134,174.25)	$ (110,763.25)	$ (244,937.50)	$ 23,198.75	$ (221,738.75)	$ (218,569.25)	$ (440,308.00)
	Budget Period 2							
	Q1		Q2		Q3		Q4	
	4/1/2014-8/15/2014		8/16/2014-12/31/2014		1/1/2015-5/15/2015		5/16/2015-9/30/2015	
	Q1	Cumulative Total	Q2	Cumulative Total	Q3	Cumulative Total	Q4	Cumulative Total
Baseline Cost Plan								
Federal Share	$ 127,422.00	$ 661,113.00	$ 127,422.00	$ 788,535.00	$ 127,422.00	$ 915,957.00	$ 127,422.00	$ 1,043,379.00
Non-Federal Share	$ 34,048.50	$ 174,275.00	$ 34,048.50	$ 208,323.50	$ 34,048.50	$ 242,372.00	$ 34,048.50	$ 276,420.50
Total Planned	$ 161,470.50	$ 835,388.00	$ 161,470.50	$ 996,858.50	$ 161,470.50	$ 1,158,329.00	$ 161,470.50	$ 1,319,799.50
Actual Incurred Cost								
Federal Share	$ -	$ 324,543.00	$ -	$ 324,543.00	$ -	$ 324,543.00	$ -	$ 324,543.00
Non-Federal Share	$ -	$ 70,537.00	$ -	$ 70,537.00	$ -	$ 70,537.00	$ -	$ 70,537.00
Total Incurred Cost	$ -	$ 395,080.00	$ -	$ 395,080.00	$ -	$ 395,080.00	$ -	$ 395,080.00
Variance								
Federal Share	$ (127,422.00)	$ (336,570.00)	$ (127,422.00)	$ (463,992.00)	$ (127,422.00)	$ (591,414.00)	$ (127,422.00)	$ (718,836.00)
Non-Federal Share	$ (34,048.50)	$ (103,738.00)	$ (34,048.50)	$ (137,786.50)	$ (34,048.50)	$ (171,835.00)	$ (34,048.50)	$ (205,883.50)
Total Variances	$ (161,470.50)	$ (440,308.00)	$ (161,470.50)	$ (601,778.50)	$ (161,470.50)	$ (763,249.00)	$ (161,470.50)	$ (924,719.50)

7 References

Archie, G.E., 1942, The Electrical Resistivity Log as an Aid in Determining Some Reservoir Characteristics.

Atik, Z., Windmeier, C., and Oellrich, L.R., 2006, Experimental Gas Hydrate Dissociation Pressures for Pure Methane in Aqueous Solutions of MgCl2 and CaCl2 and for a (Methane + Ethane) Gas Mixture in an Aqueous Solution of (NaCl + MgCl2): Journal of Chemical & Engineering Data, v. 51, p. 1862-1867.

Bily, C., and Dick, J.W.L., 1974, Naturally occurring gas hydrates in the Mackenzie Delta, N.W.T: Bulletin of Canadian Petroleum Geology, v. 22, p. 340-352.

Bishnoi, P.R., and Dholabhai, P.D., 1999, Equilibrium conditions for hydrate formation for a ternary mixture of methane, propane and carbon dioxide, and a natural gas mixture in the presence of electrolytes and methanol: Fluid Phase Equilibria, v. 158–160, p. 821-827.

Chen, Q., Liu, C., and Ye, Y., 2009, Experimental study on geochemical characteristic of methane hydrate formed in porous media: Journal of Natural Gas Chemistry, v. 18, p. 217-221.

Chen, Y.F., Matsumoto, R., Tomaru, H., and Anton, D., 2005, Organic carbon, nitrogen, sulphur and δ34S compositions of pyrite and pore waters in the JAPEX/JNOC/GSC et al. Mallik 5L-38 gas hydrate production research well, *in* Dallimore, S.R., and Collett, T.S., eds., Scientific Results from the Mallik 2002 Gas Hydrate Production Research Well Program, Mackenzie Delta, Northwest Territories, Canada, Volume Bulletin 585, Geological Survey of Canada, p. 14.

De Roo, J.L., Peters, C.J., Lichtenthaler, R.N., and Diepen, G.A.M., 1983, Occurrence of methane hydrate in saturated and unsaturated solutions of sodium chloride and water in dependence of temperature and pressure: AIChE Journal, v. 29, p. 651-657.

Dholabhai, P.D., Scott Parent, J., and Raj Bishnoi, P., 1997, Equilibrium conditions for hydrate formation from binary mixtures of methane and carbon dioxide in the presence of electrolytes, methanol and ethylene glycol: Fluid Phase Equilibria, v. 141, p. 235-246.

Eichholz, C., Majumdar, A., Clarke, M.A., Oellrich, L.R., and Bishnoi, P.R., 2004, Experimental Investigation and Calculation of Methane Hydrate Formation Conditions in the Presence of Ethylene Glycol and Sodium Chloride: Journal of Chemical & Engineering Data, v. 49, p. 847-851.

Expedition 311 Scientists, 2006, Site U1328, *in* Riedel, M., Collett, T.S., Malone, M.J., and Expedition 311 Scientists, eds., Proceedings of the Integrated Ocean Drilling Program, Volume 311: Washington, DC (Integrated Ocean Drilling Program Management International, Inc.).

Haberer, R.M., Mangelsdorf, K., Dieckmann, V., Fuhrmann, A., Wilkes, H., and Horsfield, B., 2005, Characterization of the organic matter in lignite layers of the Kugmallit Sequence (Oligocene) at the JAPEX/JNOC/GSC et al. Mallike 5L-38 gas hydrate production research well, *in* Dallimore, S.R., and Collett, T. S., ed., Scientific Results from the Mallik 2002 Gas Hydrate Production Research Well Program, Mackenzie Delta, Northwest Territories, Canada, Volume Bulletin 585, Geological Survey of Canada, p. 14.

Husebø, J., Ersland, G., Graue, A., and Kvamme, B., 2009, Effects of salinity on hydrate stability and implications for storage of CO2 in natural gas hydrate reservoirs: Energy Procedia, v. 1, p. 3731-3738.

Jager, M.D., Peters, C.J., and Sloan, E.D., 2002, Experimental determination of methane hydrate stability in methanol and electrolyte solutions: Fluid Phase Equilibria, v. 193, p. 17-28.

Jager, M.D., and Sloan, E.D., 2001, The effect of pressure on methane hydration in pure water and sodium chloride solutions: Fluid Phase Equilibria, v. 185, p. 89-99.

Kang, S.-P., Chun, M.-K., and Lee, H., 1998, Phase equilibria of methane and carbon dioxide hydrates in the aqueous MgCl2 solutions: Fluid Phase Equilibria, v. 147, p. 229-238.

Kharrat, M., and Dalmazzone, D., 2003, Experimental determination of stability conditions of methane hydrate in aqueous calcium chloride solutions using high pressure differential scanning calorimetry: The Journal of Chemical Thermodynamics, v. 35, p. 1489-1505.

Li, S., Chen, Y., and Hao, Y., 2011, Experimental study of influence factors of hot-brine stimulation for dissociation of NGH in porous media, paper presented at 7th International Conference on Gas Hydrates (ICGH 2011): Edinburgh, Scotland, United Kingdom.

Liu, C., Ye, Y., Sun, S., Chen, Q., Meng, Q., and Hu, G., 2013, Experimental studies on the P-T stability conditions and influencing factors of gas hydrate in different systems: Science China Earth Sciences, v. 56, p. 594-600.

Lu, H., Dutrisac, R., Ripmeester, J., Wright, F., and Uchida, T., 2005, Measurements of gas hydrate saturation in sediment cores recovered from the JAPEX/JNOC/GSC et al. Mallik 5L-38 gas hydrate production research well, *in* Dallimore, S.R., and Collett, T.S., eds., Scientific Results from the Mallik 2002 Gas Hydrate Production Research Well Program, Mackenzie Delta, Northwest Territories, Canada, Volume Bulletin 585, Geological Survey of Canada, p. 11.

Maekawa, T., and Imai, N., 2000, Equilibrium conditions of methane and ethane hydrates in aqueous electrolyte solutions: Annals of the New York Academy of Sciences, v. 912, p. 932-939.

Maekawa, T., Iton, S., Sakata, S., Igari, S.I., and Imai, N., 1995, Pressure and temperature conditions for methane hydrate dissociation in sodium chloride solutions: Geochemical Journal, v. 29, p. 325-329.

Masoudi, R., Tohidi, B., Danesh, A., Todd, A.C., Anderson, R., Burgass, R.W., and Yang, J., 2005, Measurement and prediction of gas hydrate and hydrated salt equilibria in aqueous ethylene glycol and electrolyte solutions: Chemical Engineering Science, v. 60, p. 4213-4224.

Matsumoto, R., Tomaru, H., Chen, Y.F., Lu, H., and Clark, I.D., 2005, Geochemistry of the interstital waters of the JPAX/JNOC/GSC et al. Mallik 5L-38 gas hydrate production research well, *in* Dallimore, S.R., and Collett, T.S., eds., Scientific Results from the Mallik 2002 Gas Hydrate Production Research Well Program, Mackenzie Delta, Northwest Territories, Canada, Volume Bulletin 585, Geological Survey of Canada, p. 11.

Medioli, B.E., Wilson, N., Dallimore, S.R., Pare, D., Brennan-Alpert, P., and Oda, H., 2005, Sedimentology of the cored interval, JAPEX/JNOC/GSC et al. gas hydrate production research well, *in* Dallimore, S.R., and Collett, T.S., eds., Scientific Results from the Mallik 2002 Gas Hydrate Production Research Well Program, Mackenzie Delta, Northwest Territories, Canada, Volume Bulletin 585, Geological Survey of Canada, p. 14.

Mei, D.-H., Liao, J., Yang, J.-T., and Guo, T.-M., 1996, Experimental and Modeling Studies on the Hydrate Formation of a Methane + Nitrogen Gas Mixture in the Presence of Aqueous Electrolyte Solutions: Industrial & Engineering Chemistry Research, v. 35, p. 4342-4347.

Mohammadi, A.H., Afzal, W., and Richon, D., 2008, Gas hydrates of methane, ethane, propane, and carbon dioxide in the presence of single NaCl, KCl, and CaCl2 aqueous solutions: Experimental measurements and predictions of dissociation conditions: The Journal of Chemical Thermodynamics, v. 40, p. 1693-1697.

Mohammadi, A.H., and Richon, D., 2009, Methane hydrate phase equilibrium in the presence of salt (NaCl, KCl, or CaCl2) + ethylene glycol or salt (NaCl, KCl, or CaCl2) + methanol aqueous solution: Experimental determination of dissociation condition: The Journal of Chemical Thermodynamics, v. 41, p. 1374-1377.

—, 2010, Gas Hydrate Phase Equilibrium in the Presence of Ethylene Glycol or Methanol Aqueous Solution: Industrial & Engineering Chemistry Research, v. 49, p. 8865-8869.

Najibi, H., Chapoy, A., Haghighi, H., and Tohidi, B., 2009, Experimental determination and prediction of methane hydrate stability in alcohols and electrolyte solutions: Fluid Phase Equilibria, v. 275, p. 127-131.

Ng, H.-J., and Robinson, D.B., 1985, Hydrate formation in systems containing methane, ethane, propane, carbon dioxide or hydrogen sulfide in the presence of methanol: Fluid Phase Equilibria, v. 21, p. 145-155.

Østergaard, K.K., Anderson, R., Llamedo, M., and Tohidi, B., 2002, Hydrate phase equilibria in porous media: effect of pore size and salinity: Terra Nova, v. 14, p. 307-312.

Saw, V.K., Ahmad, I., Mandal, A., Udayabhanu, G., and Laik, S., 2012, Methane hydrate formation and dissociation in synthetic seawater: Journal of Natural Gas Chemistry, v. 21, p. 625-632.

Sun, R., and Duan, Z., 2005, Prediction of CH4 and CO2 hydrate phase equilibrium and cage occupancy from ab initio intermolecular potentials: Geochimica et Cosmochimica Acta, v. 69, p. 4411-4424.

Takahashi, H., Fercho, E., and Dallimore, S.R., 2005, Drilling and operations overview of the Mallik 2002 Production Research Well Program, *in* Dallimore, S.R., and Collett, T.S., eds., Scientific Result.

Tang, L.G., Xiao, R., Huang, C., Feng, Z.P., and Fan, S.S., 2005, Experimental Investigation of Production Behavior of Gas Hydrate under Thermal Stimulation in Unconsolidated Sediment: Energy & Fuels, v. 19, p. 2402-2407.

Wright, J.F., Dallimore, S.R., Nixon, F.M., and Duchesne, C., 2005, In situ stability of gas hydrate in reservoir sediments of the JAPEX/JNOC/GSC et al. Mallik 5L-38 gas hydrate production research well, *in* Dallimore, S.R., and Collett, T.S., eds., Results from the Mallik 2002 Gas Hydrate Production Research Well Program, Volume 585: Mackenzie Delta, Northwest Territories, Canada, Geological Survey of Canada, p. 11.

Yang, X., Sun, C.-Y., Su, K.-H., Yuan, Q., Li, Q.-P., and Chen, G.-J., 2012, A three-dimensional study on the formation and dissociation of methane hydrate in porous sediment by depressurization: Energy Conversion and Management, v. 56, p. 1-7.

Yang, X., Sun, C.-Y., Yuan, Q., Ma, P.-C., and Chen, G.-J., 2010, Experimental Study on Gas Production from Methane Hydrate-Bearing Sand by Hot-Water Cyclic Injection: Energy & Fuels, v. 24, p. 5912-5920.

Yousif, M.H., Abass, H.H., Selim, M.S., and Sloan, E.D., 1991, Experimental and Theoretical Investigation of Methane-Gas-Hydrate Dissociation in Porous Media: SPE Reservoir Engineering, v. 6, p. 69-76.

Yousif, M.H., and Sloan, E.D., 1991, Experimental Investigation of Hydrate Formation and Dissociation in Consolidated Porous Media: SPE Reservoir Engineering, v. 6, p. 452-458.

Yuan, Q., Sun, C.-Y., Wang, X.-H., Zeng, X.-Y., Yang, X., Liu, B., Ma, Z.-W., Li, Q.-P., Feng, L., and Chen, G.-J., 2013, Experimental study of gas production from hydrate dissociation with continuous injection mode using a three-dimensional quiescent reactor: Fuel, v. 106, p. 417-424.

Yuan, Q., Sun, C.-Y., Yang, X., Ma, P.-C., Ma, Z.-W., Li, Q.-P., and Chen, G.-J., 2011, Gas Production from Methane-Hydrate-Bearing Sands by Ethylene Glycol Injection Using a Three-Dimensional Reactor: Energy & Fuels, v. 25, p. 3108-3115.

National Energy Technology Laboratory

626 Cochrans Mill Road
P.O. Box 10940
Pittsburgh, PA 15236-0940

3610 Collins Ferry Road
P.O. Box 880
Morgantown, WV 26507-0880

13131 Dairy Ashford Road, Suite 225
Sugar Land, TX 77478

1450 Queen Avenue SW
Albany, OR 97321-2198

Arctic Energy Office
420 L Street, Suite 305
Anchorage, AK 99501

Visit the NETL website at:
www.netl.doe.gov

Customer Service Line:
1-800-553-7681